Supplementary tables

Table S1. Antibodies used in this study

Antibody	catalog	Dilution	Company
For Western blotting			
EGR1	22008-1-AP	1:1000	Proteintech
N-Cadherin (D4R1H)	13116	1:1000	CST
E-Cadherin	A16811	1:1000	Abclone
CD44 (156-3C11)	3570S	1:1000	CST
Vimentin (D21H3)	5741	1:1000	CST
α-SMA	ab5694	1:500	Abcam
Bmi1 (D20B7)	6964T	1:500	CST
Nanog (D73G4)	4903	1:800	CST
Twist1	25465-1-AP	1:500	Proteintech
TGF-β1 (56E4)	3709	1:1000	CST
STAT3	10253-2-AP	1:1000	Proteintech
P-STAT3	ARE6058	1:1000	AR antibody Revolution
GAPDH (D16H11)	5174S	1:1000	CST
Secondary antibody	7076S	1:5000	CST
Secondary antibody	7074S	1:5000	CST
For Immunohistochemistry			
EGR1	22008-1-AP	1:300	Proteintech
Bmi1 (D20B7)	6964T	1:200	CST
Nanog (D73G4)	4903	1:400	CST
CD44	15675-1-AP	1:500	Proteintech
P-STAT3	ARE6058	1:100	AR antibody Revolution
Secondary antibody	Envision kit (HRP, rabbit/mouse, DAB+)	Ready-to-use	DAKO

For Immunofluorescence staining			
EGR1	22008-1-AP	1:300	Proteintech
HBME1	M3505	1:50	DAKO
HOXA11	Ab54365	1:250	Abcam
CD44	15675-1-AP	1:500	Proteintech
Ki67	GM724029	1:50	Gene Tech
TGF-β1	TA1027	1:50	Abmart
STAT3	10253-2-AP	1:200	Proteintech
P-STAT3	9145S	1:100	CST
DAPI	C1002	1:1000	Beyotime
Secondary antibody	Alexa Fluor 594 anti-mouse IgG	1:50	Invitrogen
Secondary antibody	Alexa Fluor 594 anti-rabbit IgG	1:50	Invitrogen
Secondary antibody	Alexa Fluor 488 anti-rabbit IgG	1:50	Invitrogen
Secondary antibody	Alexa Fluor 647 anti-mouse IgG	1:50	Invitrogen
Secondary antibody	Alexa Fluor 680 anti-rabbit IgG	1:50	Invitrogen

Table S2. The sequences of gene-specific primers used for qRT-PCR, vector constructs and ChIP assay

Gene name	Forward (5'-3')	Reverse (5'-3')
Primers for qRT-PCR		
EGR1	GGTCAGTGGCCTAGTGAGC	GTGCCGCTGAGTAAATGGGA
CD44s	AATCCCTGCTACCAGAGACC	TTCAGATCCATGAGTGGTATGGG
CD44v5-v8	TCCCTGCTACCAATATGGACTC	CAGAGTAGAAGTTGTTGGATGGTC
CD44v2	GCAACCAAGAGGCAAGAAA	CAGCCATTTGTGTTGTTGTGTG
CD44v3	CGTCTTCAAATACCATCTCAGC	CAATGCCTGATCCAGAAAAAC
CD44v4	TGACCACACAAAACAGAACC	GTTGTCTGAAGTAGCACTTCC
CD44v5	GAAATGGCACCACTGCTTATG	GTCTCTTCTTCCTCATGATGCT
CD44v6	AGGAACAGTGGTTTGGCAAC	CGAATGGGAGTCTTCTCTGG
CD44v7	TCAGCTCATACCAGCCATCC	TCCTTCTTCCTGCTTGATGAC
CD44v8	TCAGCCTACTGCAAATCCAA	GAGGTCCTGTCCTGTCCAAA
CD44v9	AGCAGAGTAATTCTCAGAGCTTC	TCAGAGTAGAAGTTGTTGGATGG
CD44v10	GGAATGATGTCACAGGTGGA	AGGTCACTGGGATGAAGGTC
Primers for vector constructs		
H_TGFβ1 promoter(-1900 to +100) WT	AGGTACCGAGCTCTTACGCGTC CCACCCTCACCCTACCCA	CTTACTTAGATCGCAGATCTCGAGG GGGCGTCCCCCCTGCCC
H_TGFβ1 promoter(-1900 to -183) WT	AGGTACCGAGCTCTTACGCGTC CCACCCTCACCCTACCCA	CTTACTTAGATCGCAGATCTCGAGC CCCGGCTCCGCCCCGCAA
H_TGFβ1 promoter(-1900 to +100) MT1	AGGTACCGAGCTCTTACGCGTC CCACCCTCACCCTACCCA	CTTACTTAGATCGCAGATCTCGAGG GGGCGTCCCCCCTGCCC
H_TGFβ1 promoter(-1900 to +100) MT2	AGGTACCGAGCTCTTACGCGTC CCACCCTCACCCTACCCA	CTTACTTAGATCGCAGATCTCGAGG GGGCGTCCCCCCTGCCC
H_EGR1	GCGAATTCGAAGTATACCTCGAG GCCACCATGGCCGCGGCCA	CGATCGCAGATCCTTGGATCCTTAG CAAATTTCAATTGTCCTGGGAG
Primers for ChIP		
TGF-β1	ATTAAGCCTTCTCCGCCTGGT	TCGGCAGGGGGTTTTGAAGCC

Supplementary figures and legends

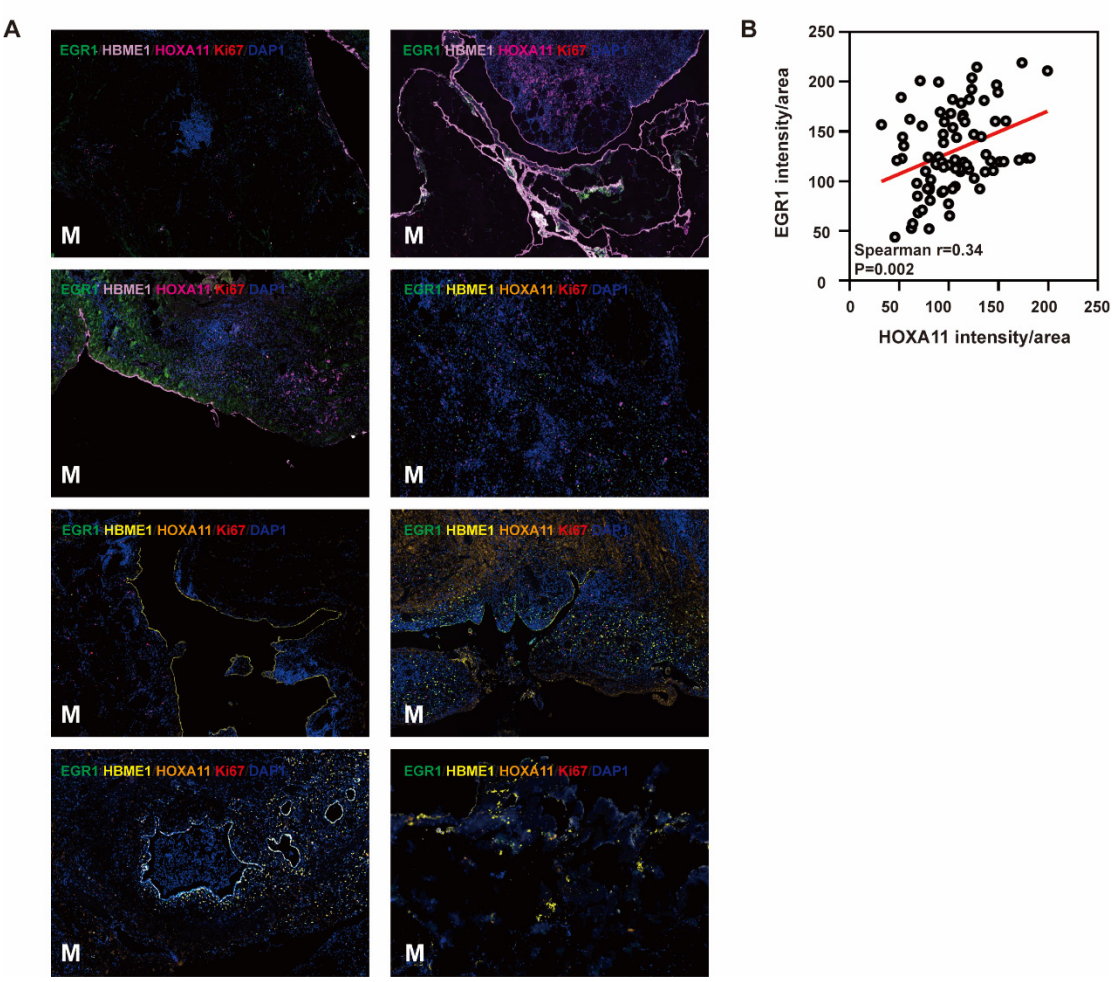

Figure S1. A. Multiple immunofluorescences staining of the PM and the matched paracancerous tissue in eight patients with GC confirmed by pathology (M: peritoneal metastasis) (n=8). B. Spearman correlation analysis of mean fluorescence intensity between HOXA11 and EGR1.

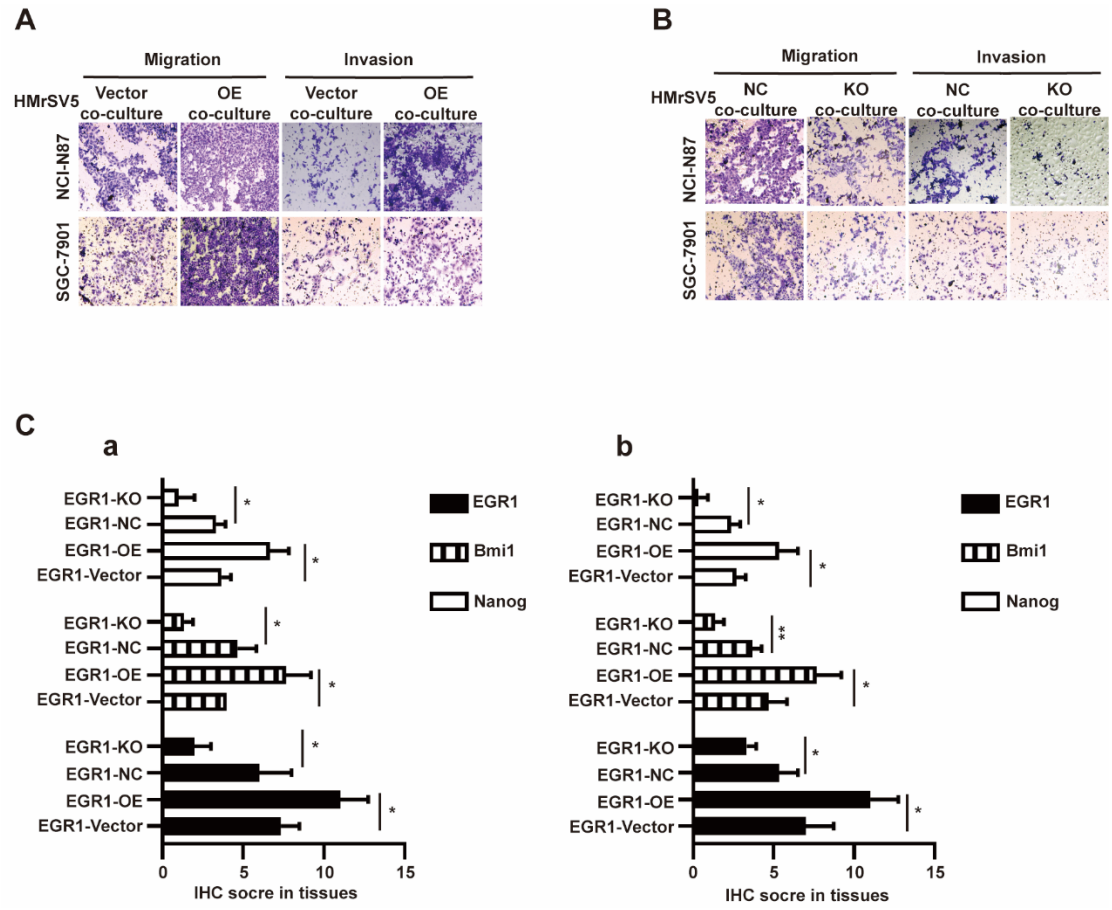

Figure S2. A-B. Cell migration and invasion were analyzed in NCI-N87 and SGC-7901 co-cultured with EGR1-overexpressing HMrSV5 cells (A) and with EGR1-knockout HMrSV5 cells (B). Ca-b. The statistical analyses of EGR1, Bmi1, and Nanog expression were evaluated by IHC score in tissues of xenografts. *, $P < 0.05$; **, $P < 0.01$.

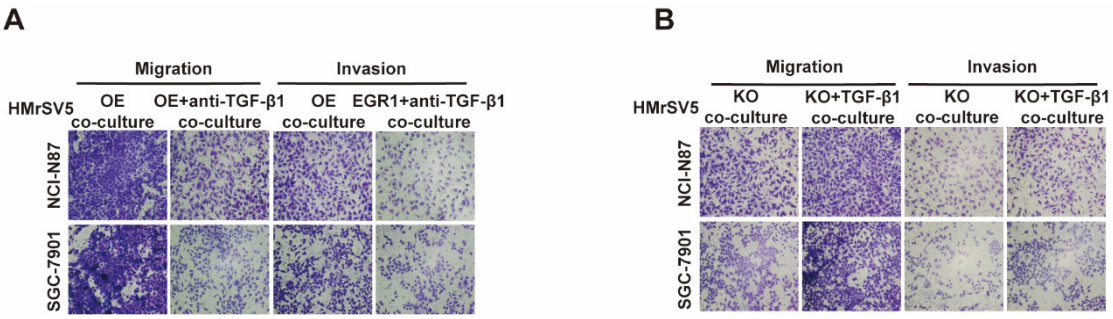

Figure S3. A-B. Cell migration and invasion were analyzed in NCI-N87 and SGC-7901 treated with TGF-β1 neutralizing antibody in EGR1-overexpressing HMrSV5 cells co-cultured system (A) and with recombinant TGF-β1 in EGR1-knockout HMrSV5 cells co-cultured system (B).

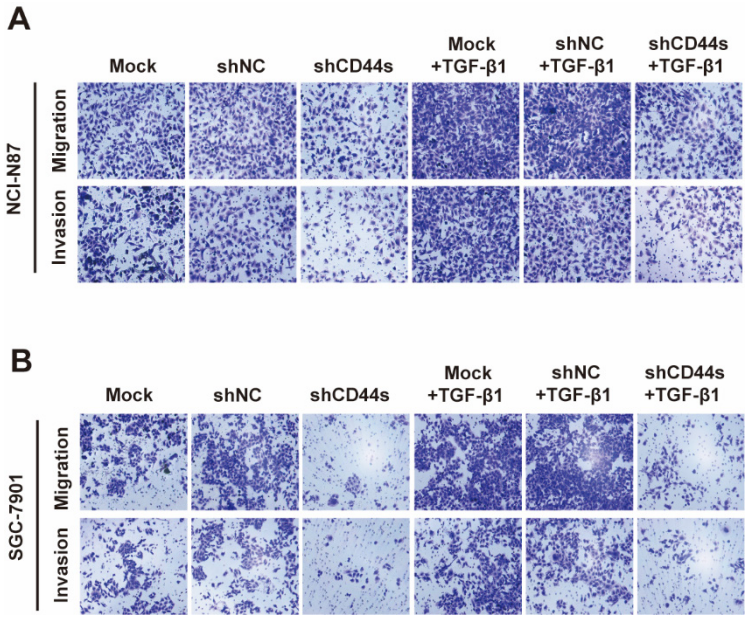

Figure S4. A-B. Cell migration and invasion were analyzed in CD44s-konckdown NCI-N87 (A) and SGC-7901 (B) cells and their respective control groups co-cultured in presence or absence of TGF-β1.

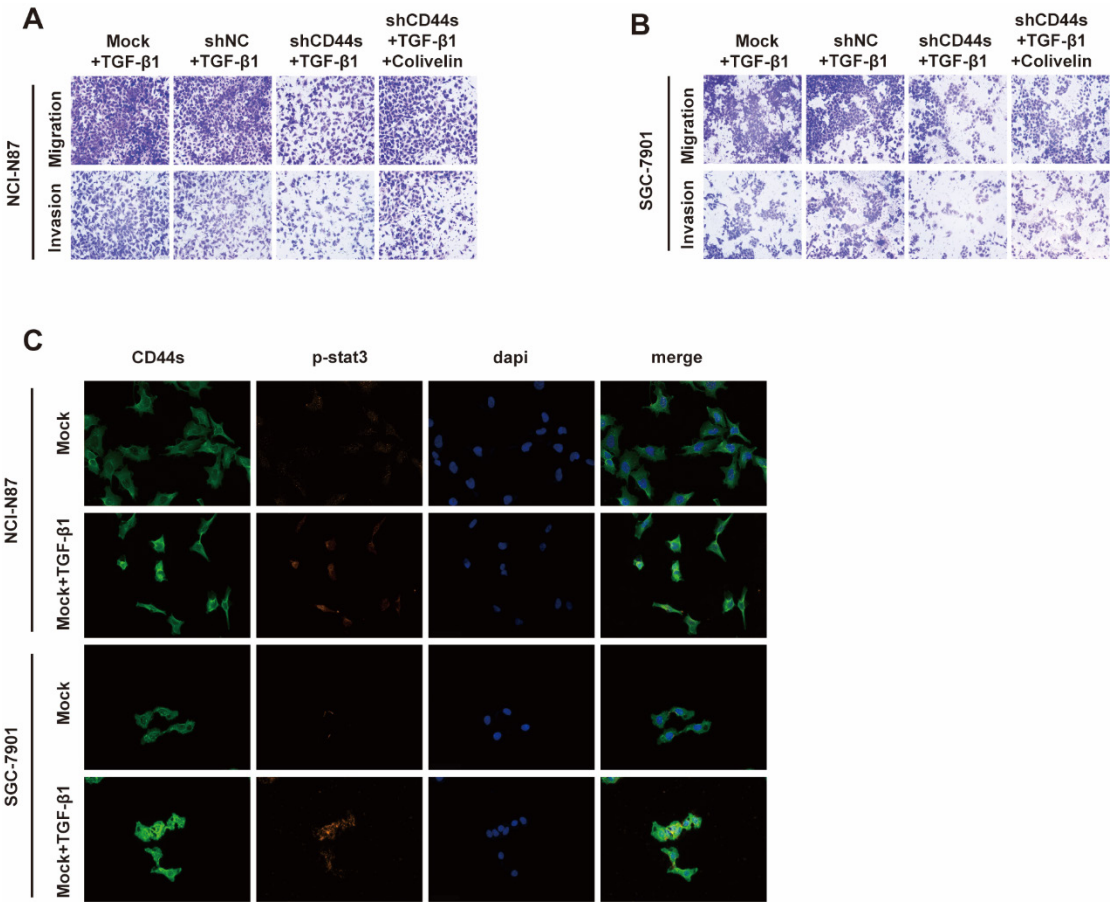

Figure S5. A-B. Cell migration and invasion were analyzed in CD44s-konckdown NCI-N87 (A) and SGC-7901 (B) cells and their respective control groups treated in presence or absence of Colivelin in TGF-β1 co-culture system. C. Immunofluorescence assay evaluating the cell internalization of CD44s and its interaction with p-STAT3 in NCI-N87 and SGC-7901 cells in the presence or absence of TGF-β1 stimulation.

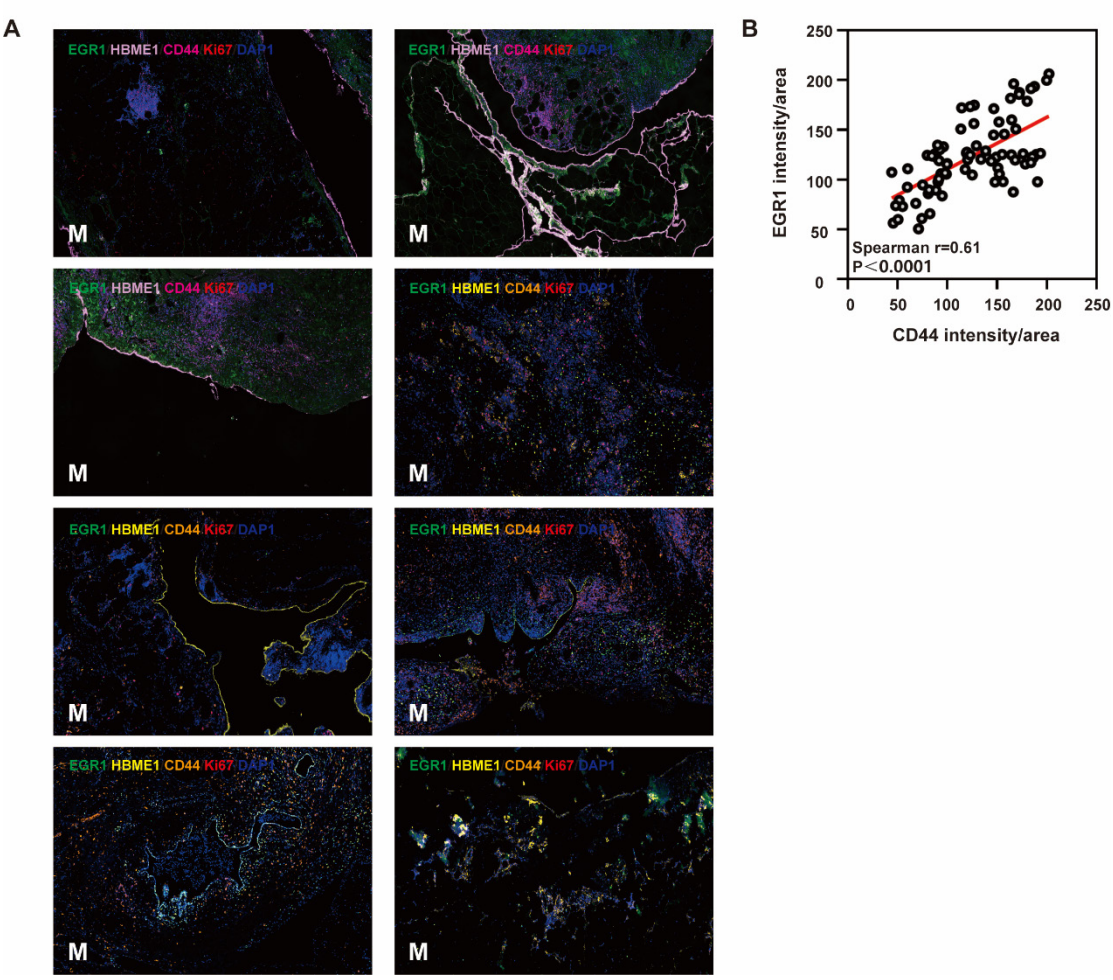

Figure S6. A. Multiple immunofluorescences staining of the PM and the matched paracancerous tissue in eight patients with GC confirmed by pathology (M: peritoneal metastasis) (n=8). B. Spearman correlation analysis of mean fluorescence intensity between CD44 and EGR1.

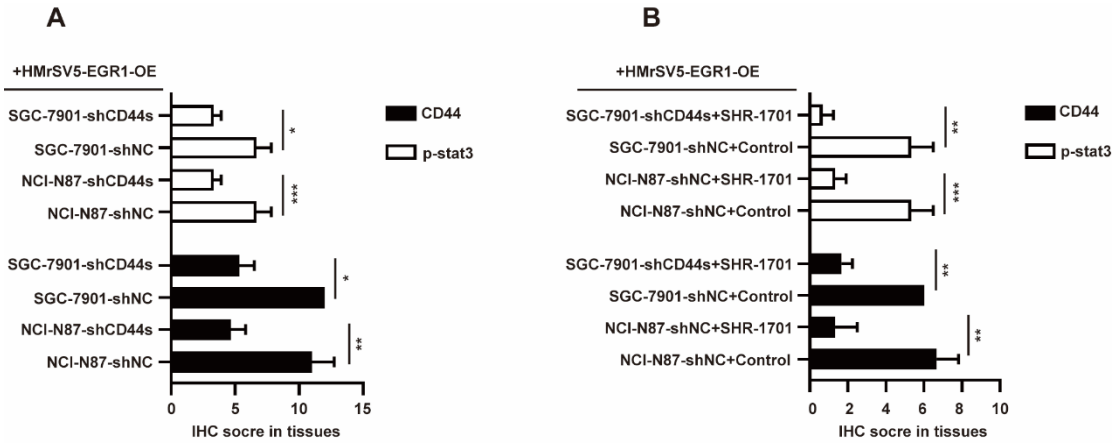

Figure S7. A-B. The statistical analyses of CD44 and p-STAT3 expression were evaluated by IHC score in tissues of xenografts. *, P < 0.05; **, P < 0.01; ***, P < 0.001.

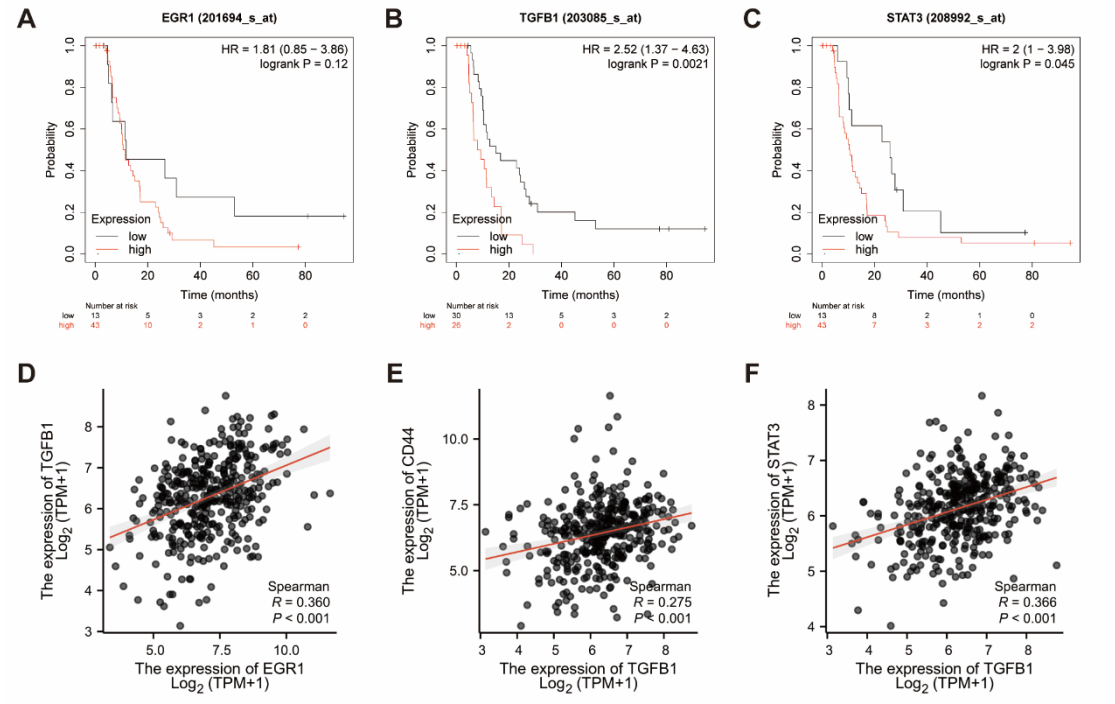

Figure S8. A-C. Kaplan-Meier survival analysis between the low and high expression groups of EGR1, TGFB1 and STAT3 in M1 stage GC tissues. D-F. Correlation analysis among EGR1, TGFB1, CD44 and STAT3 in human GC tissues based on TCGA database.